Lab Report:
Bell's Inequality and Quantum Tomography

Kutay Dengizek, Danylo Kolesnyk, Özgün Ozan Nacitarhan

Garching – December 2, 2024

Contents

1 Introduction

Over the past century, quantum mechanics has presented several counterintuitive phenomena that sharply depart from the established tenets of classical physics. Of all these peculiarities, *entanglement* stands out as one of the most intriguing and foundational aspects, placing quantum theory in direct conflict with our classical notions of locality and realism. In their seminal paper of 1935, Einstein, Podolsky, and Rosen (EPR) raised the question of whether quantum mechanics is a complete description of physical reality [4]. EPR's concerns led to the concept of *hidden variables* as possible explanations for the nonclassical correlations displayed by quantum systems.

It was not until 1964 that John Bell formulated a set of inequalities (now referred to as *Bell's inequalities*) to test if these hidden-variable theories could account for all observed quantum phenomena. Specifically, Bell's theorem shows that any local-realistic theory must obey these inequalities, whereas appropriately prepared quantum systems can violate them. Experimental violations of Bell's inequality therefore suggest that no local hidden-variable theory can fully capture the predictions of quantum mechanics.

Motivation and Aim of the Experiment

In this Advanced Laboratory Course experiment, we focus on generating and characterizing *polarization-entangled* photon pairs. The experiment is designed to address fundamental questions about quantum correlations and to explore key tools employed in modern quantum information science:

- **Generation of Entangled Photons**: Using a nonlinear optical process known as Spontaneous Parametric Down Conversion (SPDC), we create pairs of photons whose polarizations are entangled. By carefully adjusting the crystal orientation and compensators, we aim to produce one of the four *Bell states*, such as $|\phi^+\rangle = \frac{1}{\sqrt{2}}\big(|HH\rangle + |VV\rangle\big)$.

- **Measurement of Correlation Functions**: To confirm the presence of entanglement, we measure photon correlations in different polarization bases. In particular, we examine correlation functions for multiple angle settings of half-wave and quarter-wave plates. By rotating these wave plates, we can project our photonic qubits onto various polarization bases (e.g., horizontal/vertical, diagonal/antidiagonal, right/left circular). These correlation measurements are essential for characterizing entanglement and for performing quantum state tomography.

- **Violation of Bell's Inequality**: We combine the correlation measurements in carefully chosen settings to test the *Clauser-Horne-Shimony-Holt* (CHSH) form of Bell's inequality. Local hidden-variable theories demand that a certain combination of correlation values (the CHSH parameter S) does not exceed 2. Quantum mechanics, however, predicts S can reach values up to $2\sqrt{2}$. Our aim is to empirically demonstrate $S > 2$, thus ruling out local realism under the assumptions of the measurement.

- **Quantum State Tomography**: Beyond detecting the presence of entanglement, we further reconstruct the full density matrix of the generated two-photon state. Quantum tomography involves systematic measurements in a complete set of polarization bases (often taken to be X, Y, and Z for each qubit, leading to $3 \times 3 = 9$

total basis combinations). From these measurements, we retrieve the density matrix and can then quantify properties such as purity, fidelity (with respect to an ideal Bell state), and negativity (related to the Positive Partial Transpose criterion). These metrics help us evaluate the quality of our entangled source and quantify the degree of entanglement.

Structure of the Report

The sections that follow provide a detailed account of the physics background (*Qubits and Entanglement*, *Bell's Inequality*, and *Density Matrix and Quantum Tomography*). Subsequently, we describe the experimental apparatus used to generate and analyze polarization-entangled photons, including the specific steps required to observe the violation of Bell's inequality and to conduct a complete quantum state tomography. Finally, we present and discuss our measured results, comparing them with theoretical expectations. The experiment thereby serves as a practical demonstration of several core concepts in quantum information and quantum optics, connecting fundamental theory with cutting-edge applications such as quantum cryptography, teleportation, and quantum computing.

By carrying out the tasks in the experiment manual, we gain a concrete understanding of:

- How to align and optimize the nonlinear crystal setup for consistent generation of entangled photons,
- The relevance of wave plate adjustments for projecting qubits onto different measurement bases,
- Strategies for collecting and analyzing coincidence counts that confirm quantum correlations,
- And finally, how to perform the data analysis leading to Bell inequality violation and complete state reconstruction.

These goals underscore the vital role of photonic qubits in testing the foundations of quantum mechanics, as well as their importance in emerging quantum technologies.

2 Theory

2.1 Qubits and Entanglement

A **qubit** is a two-level quantum system. For photonic qubits, we commonly identify the horizontal ($|H\rangle$) and vertical ($|V\rangle$) polarizations as computational basis states:

$$|0\rangle \equiv |H\rangle\,, \quad |1\rangle \equiv |V\rangle\,.$$

Any single-qubit polarization state can be written as a superposition

$$|\psi\rangle = a\,|H\rangle + b\,|V\rangle\,,$$

with complex coefficients a and b satisfying $|a|^2 + |b|^2 = 1$. Geometrically, the state space of a single qubit can be visualized on the Bloch (or Poincaré) sphere.

Two-Qubit States. When two qubits are involved, the joint state lives in the tensor product of two 2-dimensional Hilbert spaces. A general two-qubit state can be expressed as

$$|\Psi\rangle = a_{HH}\,|HH\rangle + a_{HV}\,|HV\rangle + a_{VH}\,|VH\rangle + a_{VV}\,|VV\rangle\,.$$

If this state cannot be decomposed as a product of two single-qubit states, it is called *entangled*. One of the most famous families of entangled two-qubit states is the set of four *Bell states*:

$$\begin{aligned}
\left|\phi^+\right\rangle &= \frac{1}{\sqrt{2}}(|HH\rangle + |VV\rangle), \\
\left|\phi^-\right\rangle &= \frac{1}{\sqrt{2}}(|HH\rangle - |VV\rangle), \\
\left|\psi^+\right\rangle &= \frac{1}{\sqrt{2}}(|HV\rangle + |VH\rangle), \\
\left|\psi^-\right\rangle &= \frac{1}{\sqrt{2}}(|HV\rangle - |VH\rangle).
\end{aligned}$$

Entanglement and Local Realism. Entangled states exhibit correlations that cannot be explained by local hidden-variable theories. This fundamental nonlocality is at the heart of quantum mechanics and is what leads to the possibility of violating Bell's inequality in suitably designed experiments.

2.2 Bell's Inequality

Albert Einstein, Boris Podolsky, and Nathan Rosen originally posed the question of whether quantum mechanics provides a complete description of reality [4], suggesting the possibility that yet-to-be-discovered *hidden variables* could explain the seemingly random outcomes of quantum experiments in a deterministic, local way. In 1964, John Bell offered a way to distinguish between the predictions of such local hidden-variable (LHV) theories and the predictions of quantum mechanics. Specifically, Bell derived an inequality that any LHV model must satisfy, whereas certain *entangled* quantum states can violate it [2].

CHSH Inequality. One particularly convenient form of Bell's inequality was introduced by Clauser, Horne, Shimony, and Holt (CHSH). In this framework, each of two distant observers (often called Alice and Bob) can choose between two measurement settings, labeled a and a' for Alice, and b and b' for Bob. Each measurement yields a binary outcome denoted by ± 1. We then define the correlation coefficient

$$E(a,b) \;=\; \langle A(a)\, B(b)\rangle,$$

where $A(a)$ and $B(b)$ are the measurement outcomes (each being ± 1) for the chosen settings a and b, respectively. These correlations must satisfy the CHSH version of Bell's inequality:

$$S \;=\; \big|\, E(a,b) \;-\; E(a,b') \;+\; E(a',b) \;+\; E(a',b')\big| \;\leq\; 2.$$

A local-realistic theory cannot surpass this bound. Quantum mechanics, however, predicts that certain entangled states allow for correlations such that

$$S_{\mathrm{QM}} \;\leq\; 2\sqrt{2} \;\approx\; 2.828,$$

thus exceeding the classical limit of 2. Observing this *Bell violation* in an experiment is a strong indicator that the measured system cannot be described by any local hidden-variable model.

Correlation Functions and Measurement Settings. In practical optical experiments with photons, the observables often correspond to measuring the polarization along chosen axes. For instance, a single-qubit polarization measurement can be described by a projection onto linear polarizations (horizontal $|H\rangle$, vertical $|V\rangle$, or any rotation thereof) or onto circular polarizations (right-handed $|R\rangle$, left-handed $|L\rangle$). By adjusting wave plates and polarization beam splitters, we can implement the measurement settings a, a' (for Alice) and b, b' (for Bob). To maximize the possible violation (i.e., to achieve $S_{\mathrm{QM}} = 2\sqrt{2}$ in an ideal scenario), one typically chooses measurement directions separated by $\pm 45^\circ$ or $\pm 22.5^\circ$.

- **Example Settings for Maximum Violation**: For an entangled state such as the singlet state $|\psi^-\rangle = \frac{1}{\sqrt{2}}(|HV\rangle - |VH\rangle)$, one can choose measurement bases in the equatorial plane of the Bloch sphere at angles differing by 45°. This arrangement leads to the largest predicted quantum correlations and the maximal violation of the CHSH inequality.

In an actual experiment, one records the coincidence counts (simultaneous photon detection events) in the relevant detectors. From these, one computes empirical estimates of $E(a,b)$, $E(a,b')$, $E(a',b)$, and $E(a',b')$. Substituting these estimates into the CHSH parameter S reveals whether or not a Bell violation is observed.

2.3 Density Matrix and Quantum Tomography

Despite being derived largely for *pure states*, the theoretical arguments surrounding entanglement and Bell's inequalities are readily extended to *mixed states* through the density matrix formalism. Real-world experiments inevitably suffer from noise and imperfections, meaning that the generated states may not be perfectly pure. Hence, the density matrix ρ offers the most general description of the quantum state.

Definition and Properties. A density matrix (or density operator) ρ for a quantum state is written as:

$$\rho \;=\; \sum_i p_i \; |\phi_i\rangle \, \langle \phi_i| \, ,$$

where each $|\phi_i\rangle$ is a pure state and p_i is the classical probability associated with that pure state, satisfying $\sum_i p_i = 1$. The density matrix must obey:

- **Hermiticity**: $\rho = \rho^\dagger$.
- **Positive semi-definiteness**: $\rho \geq 0$, implying all eigenvalues are nonnegative.
- **Normalization**: $\mathrm{Tr}(\rho) = 1$.

For *pure states*, ρ can be expressed as $\rho = |\psi\rangle \langle\psi|$, and it additionally satisfies $\rho^2 = \rho$, giving $\mathrm{Tr}(\rho^2) = 1$. Mixed states have $\mathrm{Tr}(\rho^2) < 1$.

Quantum State Tomography. Tomography is the procedure by which the density matrix is experimentally reconstructed from a set of measurement outcomes. For a single qubit, one typically measures in at least three orthogonal bases (commonly the eigenbases of the Pauli matrices: X, Y, Z). For a two-qubit system, a complete tomography usually requires measurements of *both* qubits in all combinations of the X, Y, Z bases, giving nine distinct settings in total (e.g., $XX, XY, XZ, YX, \ldots, ZZ$).

From each setting, one extracts coincidence counts C_{ij} that correspond to projecting onto the basis states $|i\rangle \otimes |j\rangle$ (where i, j can be H, V, or any other basis label). Normalizing these counts yields probabilities, which in turn give the expectation values of the tensor products of Pauli matrices,

$$\langle \sigma_i \otimes \sigma_j \rangle \, .$$

Using the identity:

$$\rho \;=\; \frac{1}{4} \sum_{i,j=0}^{3} \; s_{ij} \; \sigma_i \otimes \sigma_j ,$$

where σ_0 is the 2×2 identity matrix and $\sigma_{1,2,3} \equiv (\sigma_x, \sigma_y, \sigma_z)$ are the Pauli operators, we can solve for the coefficients s_{ij} by matching them to the measured correlation values.

Entanglement Criteria: PPT and Entanglement Witnesses. Once the density matrix is reconstructed, determining whether the state is entangled is achieved by any of several criteria:

- **Positive Partial Transpose (PPT) Criterion:** For a bipartite system in a state ρ, define the partial transpose (with respect to one subsystem, say Alice) by transposing only the indices pertaining to that subsystem. If ρ is separable, this partial transpose remains a valid density matrix (i.e. it remains positive semi-definite). Conversely, if the partial transpose has at least one negative eigenvalue, then ρ is an *entangled* state. For two qubits, this PPT criterion is both necessary and sufficient.
- **Entanglement Witnesses:** An operator W is called an entanglement witness if it is constructed so that $\mathrm{Tr}(W \, \rho_{\mathrm{sep}}) \geq 0$ for *all* separable states ρ_{sep}, while $\mathrm{Tr}(W \, \rho_{\mathrm{ent}}) < 0$ for *at least one* entangled state ρ_{ent}. Thus, if the measured state

yields a negative expectation value for W, it is guaranteed to be entangled. In practice, these witnesses can be optimized for specific target states (e.g. certain Bell states) and can offer a relatively simple experimental test of entanglement.

State Characterization: Fidelity and Purity. With a reconstructed ρ at hand, we can also quantify the "closeness" to an ideal target state $|\psi\rangle\langle\psi|$ by computing the *fidelity*:

$$F(\rho, |\psi\rangle) \;=\; \langle\psi|\;\rho\;|\psi\rangle\,.$$

If ρ is pure, F reaches 1 if and only if $\rho = |\psi\rangle\langle\psi|$. More generally, the fidelity is between 0 and 1 and provides a convenient measure of how well the experimentally produced state matches the desired theoretical one.

Moreover, the *purity* of the state can be quantified via

$$\mathcal{P} \;=\; \mathrm{Tr}(\rho^2).$$

A perfectly pure state has $\mathcal{P} = 1$, whereas a completely mixed (maximally disordered) state in a d-dimensional system has $\mathcal{P} = \frac{1}{d}$.

In summary, Bell's inequality (particularly its CHSH form) and quantum tomography provide complementary ways to investigate and quantify entanglement in photonic qubits. By carefully choosing measurement bases, recording correlation functions, and reconstructing the density matrix, one can conclusively demonstrate the nonclassical, nonlocal nature of quantum mechanics.

3 Experimental Setup

In this section, the setup to test Bell's inequality and perform quantum tomography is described. The setup for generation of the entangled photons and the polarization analysis of the photons are shown in part a) and b) of Figure 1, respectively.

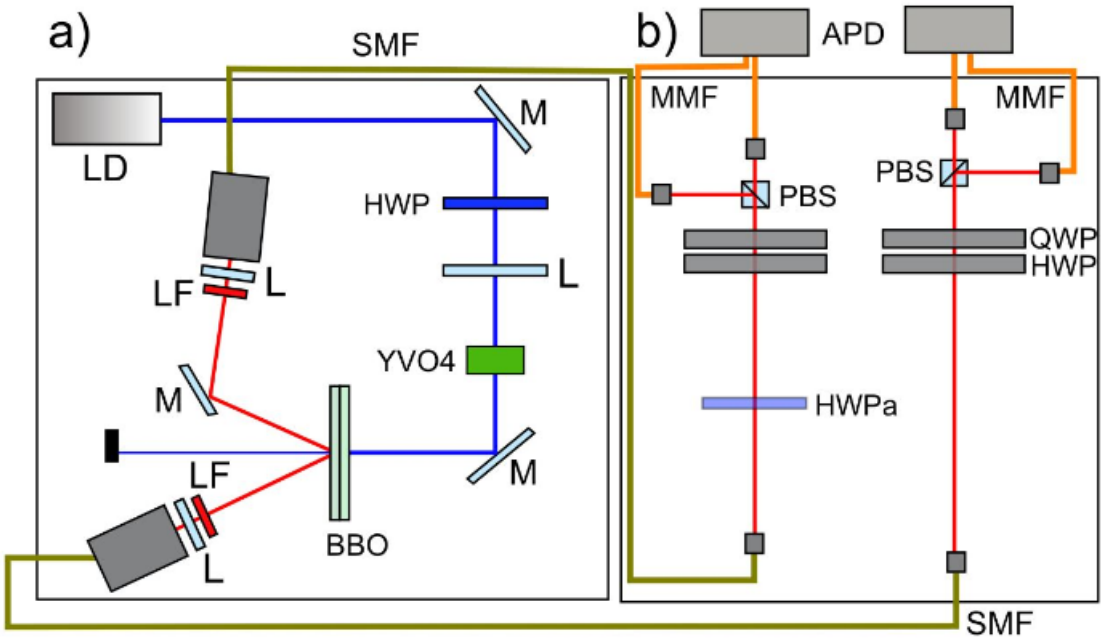

Figure 1: Schematic setup of the experiment: laser diode (LD), longpass filter (LF), half-wave plate (HWP), lens (L), Yttrium orthovanadate compensation crystal (YVO4), mirror (M), SPDC beta barium borate crystal (BBO), single-mode fiber (SMF), additional half-wave plate (HWPa), polarization beam splitter (PBS), multi- mode fiber (MMF),avalanche photodiode single photon detectors (APD).

3.1 Generation of Entangled Photons

In order to generate entangled photon pairs we levy an optical process called Spontaneous Parametric Down-Conversion (SPDC). The SPDC process is the annihilation of a pump (p) photon into the creation of two photon signal(s) and idler(i), while conserving energy and momentum in a non-linear medium which is called the phase matching conditions, Figure 2. The phase matching conditions can be classified in difference polarizations of the photons, if the three photons shave the same polarization, the SPDC is of type 0; if the signal and idler photons have the same polarization but are orthogonal to the pump polarization, it is of type I; if the signal and idler photons have perpendicular polarizations, it is of type II [5]. Momentum conservation implies that the two down converted photons are emitted in symmetric cones as in Figure 3

In the experiment the pump beam consists of a blue laser diode (labeled LD in Figure 1) with vertical polarization (V) and wavelength 404 nm. Two type-1 nonlinear crystals of Beta-barium Borate (BBO) which are optically contacted with perpendicular optical axes, Fig. 3, such that when illuminated by +45°polarized light (equal compositions of H and V) there is equal chance that a pump photon is converted in either of the crystals. In

order to polarize the pump beam to 45°, a half wave plate is used to convert the vertically polarized blue laser diode (blue HWP in Figure 1 a)).

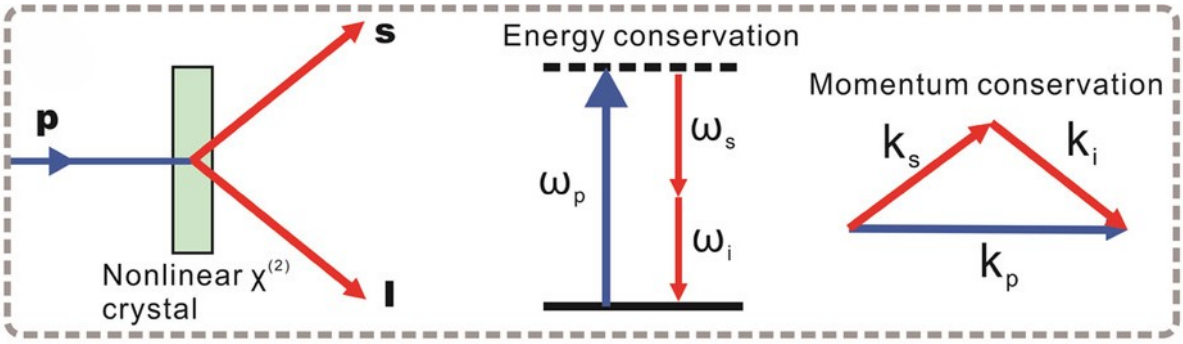

Figure 2: Schematic of SPDC process [5].

.

However, as seen in Figure 3, H and V polarized photons have a different optical path length, and can be distinguished by their detection time. Ideally, the cones in Figure 3 should perfectly align. To account for this difference, a Yttrium vanadate crystal is placed on the beam path (YV04 in Figure 1). By tilting the crystal a phase between the H and V polarizations can be created such that H and V down-converted photons have no temporal separation. In the end we produce the state:

$$\begin{aligned} |\phi\rangle &= |H, A, E_1\rangle \otimes |H, B, E_2\rangle + e^{i\phi}|V, A, E_1\rangle \otimes |V, B, E_2\rangle \\ &= |A, B\rangle \otimes |E_1, E_2\rangle \big(|HH\rangle + e^{i\phi}|VV\rangle\big) \end{aligned} \tag{1}$$

where A and B are the two spatially selected modes and E_1 and E_2 are their energies. In the next subsection,, the polarization analysis of the entangled photon pairs and how to produce other Bell states are explained.

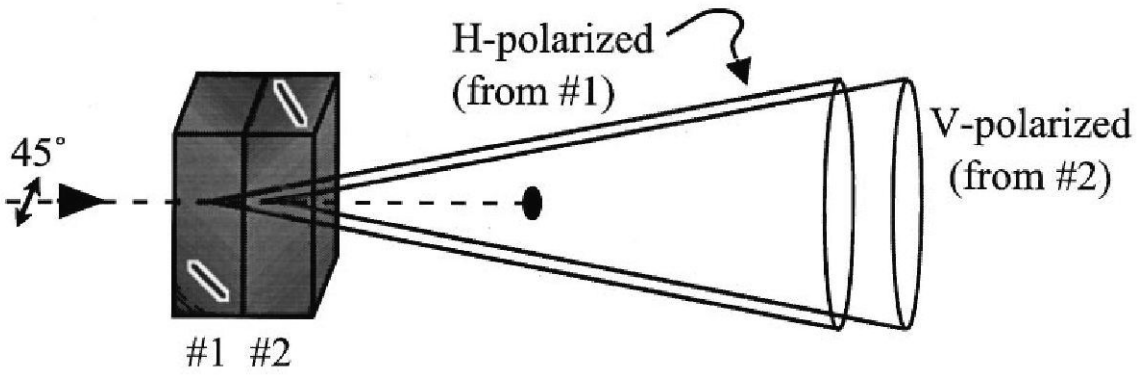

Figure 3: Two BBO crystals we use in the experiment and the production of H and V polarized photons when illuminated with a diagonally polarized light [1].

3.2 Measurement System

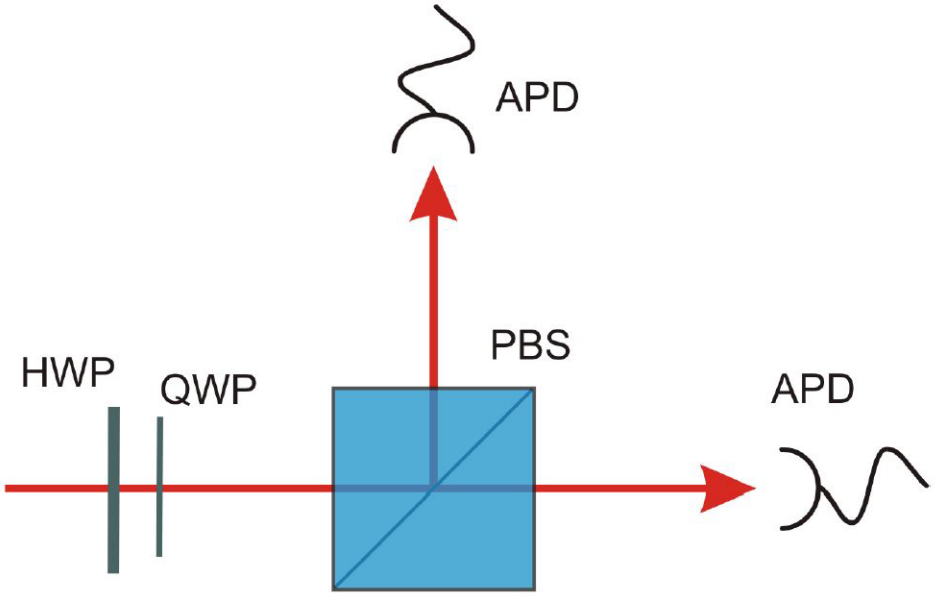

Figure 4: Polarization analysis setup for one of the arms [1]. PBS: Polarizing Beam Splitter, HWP: Half-wave plate, QWP: Quarter-wave plate, APD: Avalanche photodiode.

A polarizing beam splitter (PBS) is used to make measurements. The PBS transmits H polarized light and reflects V polarized light. Without using any wave-plates, the PBS allows us to measure polarization of the photons in the H/V basis. To measure the polarizations in other directions (left/right hand polarized or $+/-$) we use half-waveplates (HWP) and quarter-waveplates (QWP) to project those directions onto the H/V basis. For example from R to H we need a QWP with 45 degrees (HWP 0) and from + to H we need a HWP with 22.5 degrees (QWP 0). The action of the waveplates are as follows (the angles are defined relative to the H axis) :

$$\hat{\sigma}_z = \mathrm{QWP}(\alpha_{\mathrm{QWP}})\,\mathrm{HWP}(\alpha_{\mathrm{HWP}})\,\hat{\sigma}_{\theta,\phi}\,\mathrm{HWP}^{\dagger}(\alpha_{\mathrm{HWP}})\,\mathrm{QWP}^{\dagger}(\alpha_{\mathrm{QWP}}), \tag{2}$$

$$\mathrm{HWP}(\alpha_{\mathrm{HWP}}) = \begin{pmatrix} \cos(2\alpha_{\mathrm{HWP}}) & \sin(2\alpha_{\mathrm{HWP}}) \\ \sin(2\alpha_{\mathrm{HWP}}) & -\cos(2\alpha_{\mathrm{HWP}}) \end{pmatrix}. \tag{3}$$

$$\mathrm{QWP}(\alpha_{\mathrm{QWP}}) = \begin{pmatrix} \cos^2(\alpha_{\mathrm{QWP}}) - i\sin^2(\alpha_{\mathrm{QWP}}) & (1+i)\cos(\alpha_{\mathrm{QWP}})\sin(\alpha_{\mathrm{QWP}}) \\ (1+i)\cos(\alpha_{\mathrm{QWP}})\sin(\alpha_{\mathrm{QWP}}) & -i\cos^2(\alpha_{\mathrm{QWP}}) + \sin^2(\alpha_{\mathrm{QWP}}) \end{pmatrix}. \tag{4}$$

Table 1 shows the required angles of the waveplates to check correlations in different basis, X,Y,Z correspond to $+/-$, R/L, H/V basis respectively. Each entangled photon pair gets detected in 2 detectors in the basis HH,HV,VH and VV which is a coincidence event, that are used to construct the density matrix of the photon pair.

We also use an additional waveplate on one of the arms to produce other Bell states from $|\phi^+\rangle$. To rotate the Bell state $|\phi^+\rangle = \frac{1}{\sqrt{2}}(|HH\rangle + |VV\rangle)$ into the other Bell states: $|\phi^-\rangle = \frac{1}{\sqrt{2}}(|HH\rangle - |VV\rangle)$ can be achieved by placing a Half-Wave Plate (HWP) at 0° to introduce a π-phase shift. $|\psi^+\rangle = \frac{1}{\sqrt{2}}(|HV\rangle + |VH\rangle)$ can be obtained by placing a HWP at 45° to swap $|H\rangle$ and $|V\rangle$. $|\psi^-\rangle = \frac{1}{\sqrt{2}}(|HV\rangle - |VH\rangle)$ requires both a HWP at 45° and a Quarter-Wave Plate (QWP) at 90° for phase adjustment.

		HWP A	QWP A	HWP B	QWP B
X	X	22.5	0	22.5	0
X	Y	22.5	0	0	45
X	Z	22.5	0	0	0
Y	X	0	45	22.5	0
Y	Y	0	45	0	45
Y	Z	0	45	0	0
Z	X	0	0	22.5	0
Z	Y	0	0	0	45
Z	Z	0	0	0	0

Table 1: Waveplate settings for quantum state tomography of $|\phi^+\rangle$.

4 Measurement and Results

As mentioned above, this experiment has 3 different sets of measurements:

- **Measurement of Correlation Functions**
- **Violation of Bell's Inequality**
- **Quantum State Tomography**

Thus, this section is also divided into 3 different sections. Each subsection is dedicated to one of the following.

4.1 Correlation Functions

In the first part of the experiment, the aim is to measure correlation functions for 2 different cases. In both cases, there are 2 different half-wave plates. One half-wave plate (HWP_B) is located in the pathway of the photon that goes to Bob, and the other one (HWP_A) is located in the pathway of the photon that goes to Alice. The angles of the half-wave plates are as follows:

- Case 1: $\alpha_{HWP_B} = 0°$, $\alpha_{HWP_A} = i°$ ($i \in \{0, 10, 20, 30, 40, 50, 60, 70, 80, 90\}$)
- Case 2: $\alpha_{HWP_B} = 22.5°$, $\alpha_{HWP_A} = i°$ ($i \in \{0, 10, 20, 30, 40, 50, 60, 70, 80, 90\}$)

For both cases, the angles for the half-wave plates were changed by rotating the half-wave plate. After each configuration, coincidence counts were recorded by the help of a C++ script. Counts for each state and case can be seen below:

α_{HWP_A}	0°	10°	20°	30°	40°	50°	60°	70°	80°	90°
C_{HH}	251	197	164	76	29	9	28	113	187	216
C_{HV}	6	18	67	133	196	195	173	111	45	8
C_{VH}	5	8	67	135	206	232	225	127	56	7
C_{VV}	205	199	165	73	22	10	36	88	162	234

Table 2: Coincidence counts for the first case where $\alpha_{HWP_B} = 0°$.

α_{HWP_A}	0°	10°	20°	30°	40°	50°	60°	70°	80°	90°
C_{HH}	101	161	167	139	108	42	14	25	48	111
C_{HV}	105	50	26	30	76	154	190	199	155	112
C_{VH}	86	45	18	42	91	167	186	180	126	82
C_{VV}	106	183	222	199	157	98	37	21	62	135

Table 3: Coincidence counts for the second case where $\alpha_{HWP_B} = 22.5°$.

4.1.1 Calculation of Correlation Functions

To calculate the correlation values, first we need to calculate relative frequencies for each state. Relative frequencies are calculated by dividing the coincidence counts by the total number of counts:

$$f_{ij} = \frac{C_{ij}}{\sum_{i,j} C_{ij}} \quad (i, j \in \{H, V\}) \tag{5}$$

After calculating the relative frequencies, we can calculate the correlation values using the following formula with the relative frequencies from Table 2 and Table 3:

$$K_{ij}^{ex} = f_{HH} - f_{HV} - f_{VH} + f_{VV} \tag{6}$$

with $i, j \in \{H, V\}$. Correlation values for both cases can be seen below:

α_{HWP_A}	0°	10°	20°	30°	40°	50°	60°	70°	80°	90°
Case 1	0.953	0.877	0.421	-0.279	-0.775	-0.915	-0.723	-0.084	0.551	0.936
Case 2	0.040	0.567	0.797	0.648	0.227	-0.393	-0.761	-0.784	-0.437	0.118

Table 4: Calculated correlation values.

The relation between the correlation values and the angles can be visualized by plotting the correlation values against the angles. Since the correlation values are sinusoidal functions, we can fit the correlation values to a sinusoidal function. The fits for both cases can be seen below:

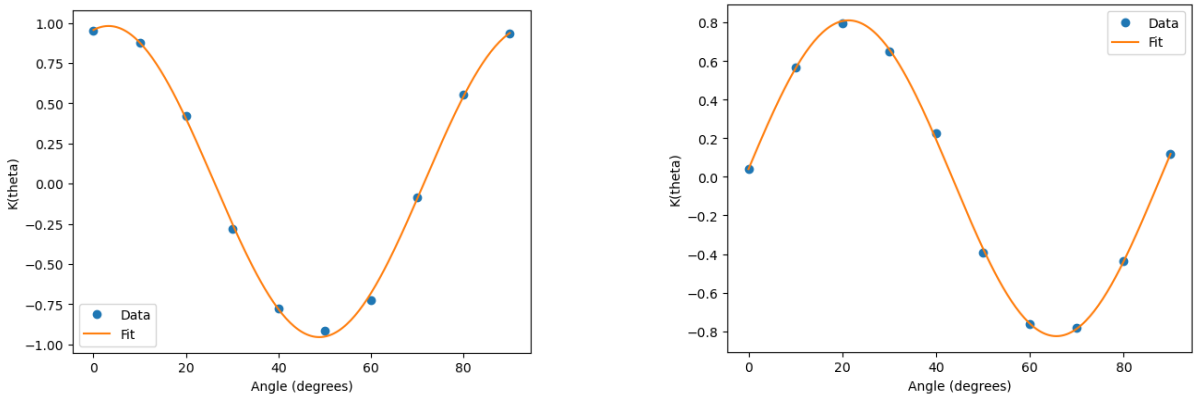

(a) Case 1.

(b) Case 2.

Figure 5: Correlation values for both cases. $f(\theta) = A \cdot \sin(B \cdot \theta + C) + D$ is used as the fit function.

4.1.2 Visibility

The visibility can be used to parameterize the contrast of measured graphs [1]. It is defined as the ratio of the difference between the maximum and minimum value of the correlation function to the sum of the maximum and minimum values. Since a correlation function can be bounded by -1 and 1, the visibility of this function would lead to $\frac{2}{0}$ in a perfect experimental setup. To deduce the visibility of the correlation function, we can use a fit function that maps a flat correlation function to 0 and a sinusoidal correlation function to 1. This can be easily achieved by using the following formula:

$$\mathcal{V} = \frac{\max_\theta \tilde{f}(\theta) - \min_\theta \tilde{f}(\theta)}{2}$$

This formula will result in a value between 0 and 1, where 0 indicates a flat correlation function and 1 indicates a correlation function varrying between -1 and 1. By using this formula, we can calculate the visibility of the correlation functions for both cases. *Case 1* has a visibility of 0.934, while *Case 2* has a visibility of 0.791.

4.1.3 Necessity of Two Correlation Functions

In this experiment, (as any other Bell test experiment) two correlation functions are needed to detect entanglement. Entanglement is a quantum correlation and to be able to detect it, we need to detect correlations (measuring correlation functions) in at least two different bases. Just measuring the correlation in one basis is not enough to detect entanglement, since correlations in one basis can be explained by classical correlations and local hidden variables[2, 3].

4.2 Violation of Bell's Inequality

In the second part of the experiment, the aim is to demonstrate the violation of CHSH inequality which is a generalization of Bell's theorem[3]. As in the first part of the experiment here we also have one half-wave plate for each party. Unlike the first part, we only have 2 different HWP angles for each party. The coincidence counts were recorded for each of the 4 possible combinations of the angles. The angles are as follows:

Alice		Bob	
α	α'	β	β'
22.5°	0°	11.25°	−11.25°

Table 5: Measurement settings for Alice and Bob.

The aim of this part is to show that the CHSH inequality is violated. The CHSH inequality is defined as follows[3]:

$$|S| \leq 2 \tag{7}$$

where

$$S = E(\alpha, \beta) + E(\alpha, \beta') + E(\alpha', \beta) - E(\alpha', \beta') \tag{8}$$

The experimental estimation of the correlations are calculated as follows:

$$E(\alpha, \beta) = \frac{C_{HH}(\alpha, \beta) - C_{HV}(\alpha, \beta') - C_{VH}(\alpha', \beta) + C_{VV}(\alpha', \beta')}{C_{HH}(\alpha, \beta) + C_{HV}(\alpha, \beta') + C_{VH}(\alpha', \beta) + C_{VV}(\alpha', \beta')} \tag{9}$$

which is exatly the same as the Equation 6. By using these experimental estimations, we can calculate the CHSH value and show that it is greater than 2. We assume that the coincidences follow Poisson distribution and the total number of counts is constant. By using these assumptions, we can calculate the the CHSH value and the error propagation. The experimental CHSH value is calculated as 2.385 ± 0.015 which is greater than the theoretical maximum value of 2 for classical correlations. This result shows that the CHSH inequality is violated and the system is entangled. However, this result is smaller than the theoretical maximum value of $2\sqrt{2} \approx 2.828$ for quantum correlations. This difference can be explained by the imperfections in the experimental setup.

4.3 Quantum State Tomography

In the last part of the experiment, the aim is to do a quantum state tomography for each of the Bell states. The angles of the waveplates and the correspğonding transformations are given in Section 3.2. As discussed in the Section 2.3, the density matrix of the Bell states can be calculated by using the coincidence counts. The experimentally constructed density matrices for the Bell states are as follows:

$\lvert\phi^+\rangle$
$\begin{pmatrix} 0.48+0.00i & 0.00+0.01i & -0.06+0.03i & 0.40+0.07i \\ 0.00-0.01i & 0.02+0.00i & 0.00+0.03i & 0.06-0.03i \\ -0.06-0.03i & 0.00-0.03i & 0.02+0.00i & -0.00-0.01i \\ 0.40-0.07i & 0.06+0.03i & -0.00+0.01i & 0.48+0.00i \end{pmatrix}$
$\lvert\phi^-\rangle$
$\begin{pmatrix} 0.47+0.00i & 0.04-0.01i & 0.08-0.05i & -0.34-0.12i \\ 0.04+0.01i & 0.03+0.00i & 0.01-0.02i & -0.08+0.05i \\ 0.08+0.05i & 0.01+0.02i & 0.03+0.00i & -0.04+0.01i \\ -0.34+0.12i & -0.08-0.05i & -0.04-0.01i & 0.47+0.00i \end{pmatrix}$
$\lvert\psi^+\rangle$
$\begin{pmatrix} 0.03+0.00i & 0.05-0.04i & 0.05-0.05i & 0.01-0.04i \\ 0.05+0.04i & 0.47+0.00i & 0.40+0.07i & -0.05+0.05i \\ 0.05+0.05i & 0.40-0.07i & 0.47+0.00i & -0.05+0.04i \\ 0.01+0.04i & -0.05-0.05i & -0.05-0.04i & 0.03+0.00i \end{pmatrix}$
$\lvert\psi^-\rangle$
$\begin{pmatrix} 0.06+0.00i & 0.10-0.03i & -0.15+0.07i & 0.02-0.01i \\ 0.10+0.03i & 0.44+0.00i & -0.37-0.10i & 0.15+0.07i \\ -0.15-0.07i & -0.37+0.10i & 0.44+0.00i & -0.10+0.03i \\ 0.02+0.01i & 0.15-0.07i & -0.10-0.03i & 0.06+0.00i \end{pmatrix}$

Table 6: Experimentally constructed density matrices of the Bell states.

As discussed in the Section 2.3, we can calculate the fidelity, purity and eigenvalues of the density matrices and prove entanglement using the PPT criterion and entanglement witnesses. The calculated values for the reconstructed Bell states are as follows:

Bell State	Purity	Fidelity	Eigenvalues
$\|\phi^+\rangle$	0.80	0.88	(0.89, 0.10, 0.04, -0.04)
$\|\phi^-\rangle$	0.71	0.80	(0.85, 0.16, 0.03, -0.04)
$\|\psi^+\rangle$	0.78	0.87	(0.89, 0.08, 0.06, -0.03)
$\|\psi^-\rangle$	0.78	0.80	(0.90, 0.14, 0.01, -0.05)

Table 7: Purity and fidelity and eigenvalues of the reconstructed Bell states.

Reconstructed density matrices have negative eigenvalues, thus they are not positive semidefinite, which means that they are not physical states. This is also due to the imperfections in the experimental setup. Another issue is that reconstructed density matrices have different eigenvalues than the theoretical ones. Any physical pure state has only one non-zero eigenvalue which is equal to 1 and Bell states are pure states. Thus, the reconstructed density matrices are not pure states. The purity of the reconstructed density matrices are also less than 1.

4.3.1 Entanglement Verification of $|\phi^+\rangle$ with PPT Criterion

PPT criterion states that if the partial transpose of the density matrix is positive semidefinite, then the state is separable. Conversely, if the partial transpose has at least one negative eigenvalue, then the state is an entangled state. The partial transpose of the reconstructed $|\phi^+\rangle$ is as follows:

$$|\phi^+\rangle^{T_B} = \begin{pmatrix} 0.48+0.00i & 0.00+0.01i & -0.06+0.03i & 0.00-0.03i \\ 0.00-0.01i & 0.02+0.00i & 0.40-0.07i & 0.06+0.03i \\ -0.06-0.03i & 0.40+0.07i & 0.02+0.00i & -0.00-0.01i \\ 0.00+0.03i & 0.06-0.03i & -0.00+0.01i & 0.48+0.00i \end{pmatrix} \tag{10}$$

The eigenvalues of the partial transpose are (-0.39, 0.39, 0.46, 0.54) which means that the state is entangled.

4.3.2 Entanglement Verification of $|\phi^+\rangle$ with Entanglement Witnesses

As discussed in the Section 2.3, an entanglement witness is a Hermitian operator that has a negative expectation value for entangled states and entanglement witnesses can be optimized to detect entanglement in a specific state. The optimized entanglement witness for the $|\phi^+\rangle$ state is as follows:

$$W = \frac{1}{2}I - |\phi^+\rangle\langle\phi^+| \tag{11}$$

The expectation value of the entanglement witness for the reconstructed $|\phi^+\rangle$ state is $Tr(W|\phi^+\rangle\langle\phi^+|) = -0.38$ which is less than 0, thus the state is entangled.

5 Discussion

This experiment aimed and suceeded to create and analyze entangled photon pairs using the four Bell states ($|\phi^+\rangle$, $|\phi^-\rangle$, $|\psi^+\rangle$, and $|\psi^-\rangle$). Additionally, the violation of Bell's inequality through the CHSH parameter demonstrates the presence of non-classical correlations.

For $|\phi^+\rangle$, we achieved the highest fidelity 0.8817 and a purity of 0.7973, which suggests that this state was prepared with great accuracy. $|\psi^+\rangle$ also showed high fidelity 0.8710 and a similarly strong purity 0.7837. The partial transpose of the density matrix of all the states had negative eigenvalues which show that they are entangled states. On the other hand, $|\phi^-\rangle$ and $|\psi^-\rangle$ had slightly lower fidelities (0.8085 and 0.8039, respectively) and purities (0.7080 and 0.7838). This is likely due to small imperfections in the alignments using waveplates or the crystals.

The CHSH parameter we measured in the experiment is $S = 2.385 \pm 0.015$. This exceeds the classical limit of $S = 2$,which violates Bell's inequality. This validates the presence of entanglement and non-classical correlations in the photon pairs.

Some of the key factors that could explain the lower fidelities and purities observed include:

- Photon loss in the optical components and during coupling to the fibers.
- Limited quantum efficiency of the Spontaneous Parametric Down Conversion process.
- Detector inefficiencies, such as dead time or recovery time or shot noise, reducing accurate photon detection.
- Misalignments in the waveplates or crystals, introducing phase and polarization errors.

High-quality Bell states are essential for a range of quantum technologies, including quantum communication protocols like quantum key distribution and teleportation. Violating Bell's inequality is one of the foundational tests of quantum mechanics. Entangled photon pairs have correlations which rule out local realistic theories such as hidden variable theories that allow for a local and realistic description of the universe.

6 Conclusion

In this experiment we successfully generated and characterized polarization entangled photon pairs using parametric down-conversion process and demonstrated the non-classical nature of the quantum correlations. By preparing the four Bell states and measuring the coincidence counts, we observed visibilities and fidelity values that are consistent with the theoretical predictions. The measured CHSH parameter of 2.385 ± 0.015 is greater than the classical limit of 2, which confirms the presence of quantum correlations in the system.

Additionally, the state tomography of the generated states was performed and allowerd us to reconstruct the density matrix of the generated states. Although the experimental imperfections lowered overall fidelity and purity, the partial transpose of the reconstructed density matrices were not positive definite, which is a clear indication of entanglement by the PPT criterion. Overall, these results confirm that the photonic systems provide an accessible platform for studying quantum correlations and entanglement.

References

[1] Lab course: Bell's inequality and quantum tomography. *Max Planck Institute of Quantum Optics*, 2020.

[2] J. S. Bell. On the einstein podolsky rosen paradox. *Physics Physique Fizika*, 1(3):195–200, Nov. 1964.

[3] J. F. Clauser, M. A. Horne, A. Shimony, and R. A. Holt. Proposed experiment to test local hidden-variable theories. *Physical Review Letters*, 23(15):880–884, Oct. 1969.

[4] A. Einstein, B. Podolsky, and N. Rosen. Can quantum-mechanical description of physical reality be considered complete? *Physical review*, 47(10):777, 1935.

[5] C. Zhang, Y.-F. Huang, B.-H. Liu, C.-F. Li, and G.-C. Guo. Spontaneous parametric down-conversion sources for multiphoton experiments. *Advanced Quantum Technologies*, 4(5):2000132, 2021.